Journal of Metals, Materials and Minerals, 36(1), e2467, 2026

Degradation of wastewater by Advanced Oxidation Processes using green synthesised CuO nanoparticles

Srinivasan VISHAL[1], Anand SARVESVARON[1], Muralidharan KEERTHANA[1], Hemanth Sanjay REDDY[1] and A Babu PONNUSAMI[1,*]

[1] *School of Chemical Engineering, Vellore Institute of Technology, Katpadi, Vellore, Tamil Nadu, Pin 632014, India*

***Corresponding author e-mail**: ababuponnusami@vit.ac.in

Received date:
12 July 2025
Revised date:
15 August 2025
Accepted date:
16 November 2025

Keywords:
Nanoparticles;
Response surface methodology;
Brown G;
Photocatalyst

Abstract

This study highlights the green synthesis of CuO nanoparticles using coconut coir extract and evaluates their photocatalytic performance in the degradation of the Brown G dye. The CuO nanoparticles were synthesised through sol-gel method, and the biomolecules like polyphenols, tannins and flavonoids acted as reducing agents to stabilise the nanoparticles. The characterisation of these nanoparticles was carried out through XRD, FTIR and FESEM methods. The nanoparticles were used to degrade the dye Brown G under UV irradiation. Response surface methodology was used to optimise the operating parameter with Box-Behnken design, which is the most suitable for varying 3 or more parameters. The parameters varied in this experiment were temperature, catalyst loading and pH. The maximum dye degradation of 80.01% was achieved under the optimised conditions of pH 7, temperature 33.5°C and at 17.5 mg of CuO catalyst. The kinetic studies of experimental data indicate that the degradation follows a first-order reaction. The results show that the green-synthesised CuO nanoparticles are an effective photocatalyst for treating dye wastewater.

1. Introduction

The release of untreated industrial effluents, especially from textile and leather processing units, has become a significant environmental concern. These effluents often contain synthetic dyes like Brown G, which are chemically stable, non-biodegradable, and harmful to both aquatic ecosystems and human health. Even at low concentrations, these dyes can block sunlight penetration in aquatic systems, reducing photosynthetic activity and depleting oxygen levels, which disrupts aquatic life. Some dyes are also carcinogenic and mutagenic, posing risks to human health when they contaminate drinking water sources. Traditional treatment approaches, such as coagulation or adsorption, are often insufficient in fully eliminating such contaminants [1,2].

Beyond environmental damage, untreated wastewater threatens human health by contaminating drinking water sources and entering the food chain through bioaccumulation [2]. Exposure to synthetic dyes has been associated with allergic reactions, skin irritation, and even carcinogenic effects [3]. Therefore, there is a growing necessity to develop advanced, efficient, and eco-friendly methods to treat dye-laden wastewater, aiming for complete mineralisation of pollutants rather than simple removal or dilution [4].

To address this challenge, Advanced Oxidation Processes (AOPs) have emerged as a viable solution due to their ability to generate highly reactive species that can mineralise complex organic compounds. Among various catalysts used in AOPs, copper oxide (CuO) nanoparticles offer advantages, including low cost, high surface reactivity, and efficient photon absorption properties [5,6]. Even though numerous plant and leaf extracts have been used to synthesise CuO nanoparticles before, the properties and chemical characteristics of Coconut coir extract, a low-cost biowaste resource, for this specific use case have not been tested before. In this study, Coconut coir extract has been used for the first time as a natural reducing and stabilising agent for synthesising Copper Oxide nanoparticles.

In the present study, CuO nanoparticles were synthesised through a green sol-gel route, utilising coconut coir extract as a natural reducing and stabilising medium. The biosynthesised nanoparticles were characterised using analytical techniques such as X-ray diffraction (XRD), Fourier Transform infrared spectroscopy (FTIR), Field emission scanning electron microscopy (FESEM), and UV-Visible spectroscopy. Their effectiveness was tested by evaluating the photocatalytic degradation of Brown G dye under UV light. Process optimisation was carried out using Response Surface Methodology (RSM) to optimise the operating parameter, and experimental data were fitted with first-order and second-order kinetics.

2. Materials and methods

2.1 Preparation of coconut coir extract

5 g of dried coconut coir was added to 250 mL of distilled water and boiled for 45 min at a temperature of 60°C. The extract was then filtered using Whatman filter paper and stored in a refrigerator for further use [5].

2.2 Preparation of CuO catalyst

4 g of $CuSO_4$ solution was added to the 50 mL of coconut coir extract, and the mixture was stirred using a magnetic stirrer at 300 rpm. After stirring, the mixture is centrifuged at 6000 rpm for 15 min, followed by two 5 min cycles at 3000 rpm with ethanol as solvent, to minimise organics present in the sample. The filtered solids were heated in the hot air oven for 3 h at 100°C [7].

2.3 Preparation of CuO nanoparticles

The green synthesis of copper oxide (CuO) nanoparticles (NPs) was carried out using $CuSO_4$ salt solution. Meanwhile, a bio-extract is generated by boiling coconut coir in distilled water, resulting in a solution rich in natural reducing agents like phenolics, flavonoids, and proteins [8]. When the copper salt solution is combined with the plant extract, the biomolecules from the extract interact with the Cu^{2+} ions. These biomolecules assist in the reduction of Cu^{2+} to either copper(I) oxide (Cu_2O) or elemental copper (Cu°). Following this, oxidation processes transform the intermediate product into copper (II) oxide (CuO). The bio-compounds not only serve as reducing agents but also act as stabilisers, capping the nanoparticles and preventing them from clumping together [2,8]. The produced CuO nanoparticle was washed with ethanol multiple times to remove organic residues. Then, the particles were dried at 250°C to remove the remaining residues and water content. The dried CuO nanoparticles were characterised and used for the photocatalytic degradation process [9]. This environmentally friendly method yields stable CuO nanoparticles that are suitable for various applications, including environmental remediation.

2.4 Preparation of synthetic dye and photocatalyst suspension

Synthetic dye (Brown -G) stock solution was prepared by adding 25 mg of Brown-G dye into 250 mL of distilled water and mixing thoroughly. From the stock solution, different concentrations of dye solution were prepared, and a specific amount of CuO catalyst was added and stirred in the dark conditions for 30 min to reach adsorption-desorption equilibrium between the catalyst and the dye. Then, the solution was exposed under the UV light source for photocatalytic degradation studies for 1 h. The UV wavelength range was measured at 100 nm to 400 nm. Aliquot samples were collected every 10 min to find the percentage dye degradation [10,11].

2.5 Dye degradation mechanism

When the synthetic dye solution with CuO catalyst was exposed to UV irradiation, CuO nanoparticles absorbed photons, leading to the excitation of electrons from the valence band (VB) to the conduction band (CB), thus generating electron-hole pairs (e^-/h^+). These charge carriers trigger redox reactions on the surface of the nanoparticles. The photogenerated holes (h^+) in the valence band can oxidise water (H_2O) or hydroxide ions (OH^-) to create highly reactive hydroxyl radicals ($^{\bullet}OH$) [12]. The electrons in the conduction band (e^-) reduce dissolved oxygen (O_2) to yield superoxide radicals ($^{\bullet}O_2^-$). Both types of radicals are essential in breaking down the intricate structure of dye molecules into simpler and less harmful substances like CO_2 and H_2O. Furthermore, in the presence of hydrogen peroxide (H_2O_2) an AOP is also activated [13]. An advanced oxidation process (AOP) is also activated. CuO serves as a catalyst in the decomposition of H_2O_2, producing additional $^{\bullet}OH$ radicals through Fenton-like reactions, which further increases the degradation rate. The basic degradation reaction mechanism is shown in Equation (1).

$$\text{Brown G dye} + {}^{\bullet}OH/{}^{\bullet}O_2^- \rightarrow \text{Degraded products } (CO_2, H_2O, \text{etc.}) \quad (1)$$

The percentage dye degradation is calculated as per the Equation (2).

$$\%\ \text{dye degradation} = \frac{C_i - C_f}{C_i} \times 100 \quad (2)$$

Where C_i = Initial dye concentration, C_f = Final dye concentration

3. Results and discussion

3.1 X-Ray diffraction analysis

The CuO nanoparticles were characterised by XRD, and the results are shown in Figure 1(a). From the results, it was observed that the notable peaks at 2θ values of 36° and 39°. These peaks correspond to CuO nanoparticles, confirming its presence [2,8]. This can be verified by referring to the JCPDS corresponding to CuO (JCPDS 48-1548).

3.2 FTIR analysis

The FTIR analysis of CuO nanoparticles is shown in Figure 1(b). The X-axis denotes wavenumber, and the Y-axis denotes transmittance [14]. The wavenumber is defined as the reciprocal of the wavelength, and transmittance is given by the ratio of the intensity of the light transmitted to that of the light incident on the surface. Following is the data of all the bonds corresponding to the attained peaks: 439.77 cm^{-1}, 547.78 cm^{-1} and 590.22 cm^{-1} for Metal-Oxygen strong bond, 798.53 cm^{-1} for C=C bending (Alkene) bond, 860.25 cm^{-1} for C–H bending, 1064.71 cm^{-1} for C–O stretching, 1612.49 cm^{-1} for C=C stretching, and 3120.82 cm^{-1} for O–H stretching. From the figure, it can be observed that the peaks observed at 439.77 cm^{-1}, 547.78 cm^{-1}, and 590.22 cm^{-1} indicate the presence of CuO NPs [7]. The bonds that correspond to Alkene (C=C), C–H bending and O–H stretching indicate the presence of bioactive compounds such as flavonoids, polyphenols and alkaloids that act as natural reducing and stabilising agents. These compounds do not interfere with the photocatalytic activity [7].

3.3 FESEM image analysis

The FESEM images of synthesised CuO nanoparticles are shown in Figure 1(c-d). From the figures, it can be observed that the particles are spherical in shape, and remain segregated from each other in small clusters. From the figure, the particles appear to be in the range of micro- to nanoscale. It can be observed that a few particles are agglomerated, forming clusters and irregular lumps in the imaging. This may be due to the presence of a few carbon compounds in the catalyst [7,15].

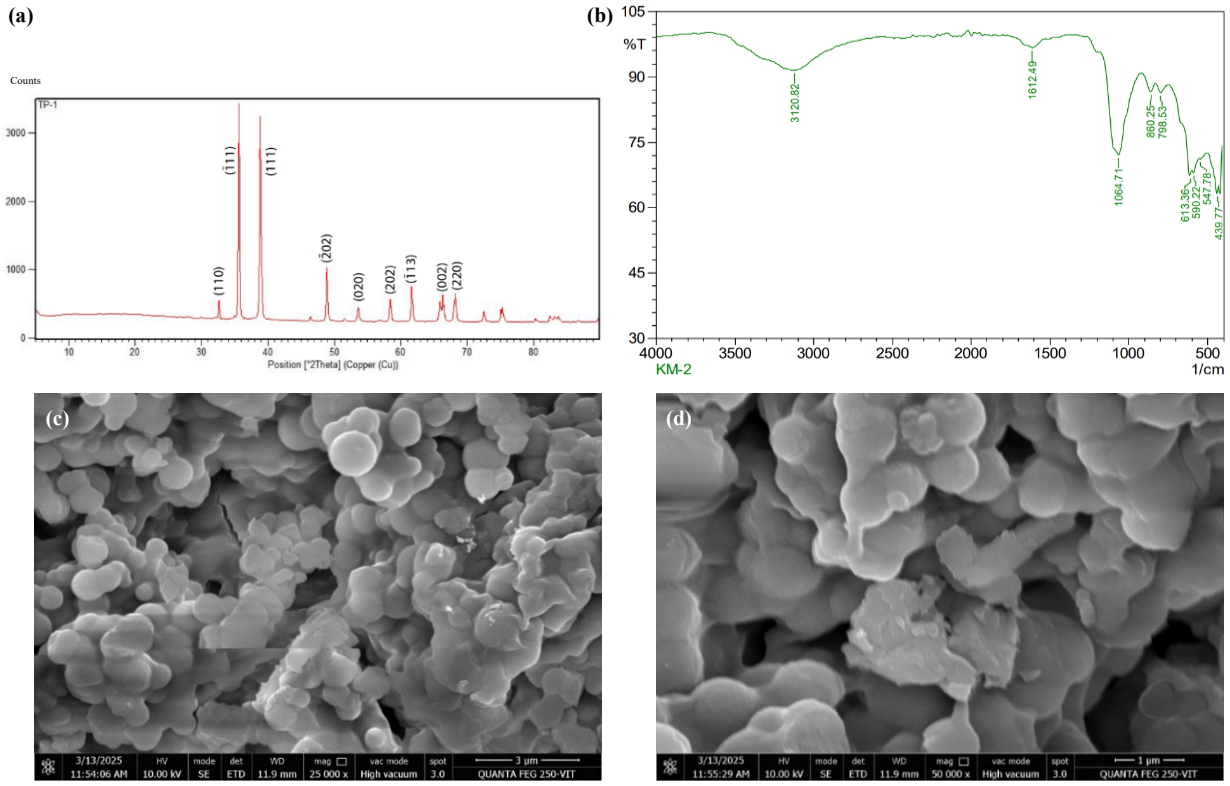

Figure 1. Characterisation of CuO Nanoparticles: (a) XRD Analysis, (b) FTIR Analysis, (c) FESEM image of CuO Nanoparticles – 3 µm scale, and (d) FESEM image of CuO Nanoparticles – 1 µm scale.

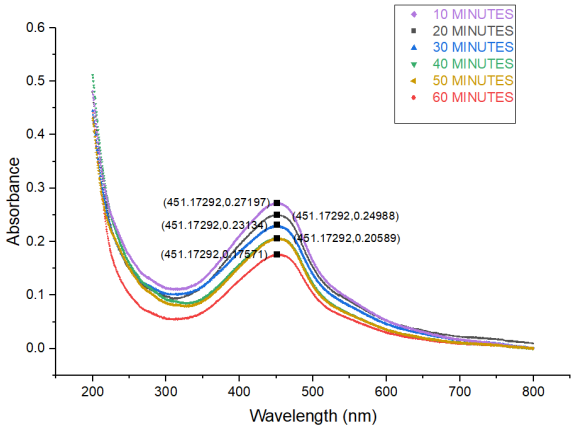

Figure 2. UV Visible spectrum for sample at various time intervals.

3.4 UV-Vis spectrophotometry

The UV-Vis spectrophotometry of synthetic dye (Brown G) wastewater was taken as continuous spectra, and the results are shown in Figure 2. During the degradation experiment, samples were taken at different time intervals and subjected to UV-Vis spectrophotometry. Absorbance values at a wavelength of 451 nm were noted down, and corresponding concentrations were calculated [16].

3.5 Response surface methodology (RSM)

The operating parameters, such as temperature, pH and catalyst dosage, were varied according to the different sets of suggested values given by the RSM Software. The Box-Behnken Design method was used to analyse and form the model for the given set of experiments, and the results were shown in Table 1. RSM gives us a detailed set of results, which helps us to compare the predicted values of degradation and the actual values of degradation obtained through experimental runs [17,18].

For a stable model, the calculated Regression value should be > 99% for the given model. The results obtained from the simulation model prove that the model formed through our experimental runs is stable (R^2 = 99.77%, R^2 predicted = 99.98%) [19].

The concentration vs time graph of run 14 is shown in Figure 5 at where the maximum degradation efficiency of 80.01% was obtained at an optimum operating condition of pH = 7, catalyst dosage = 17.5 mg, and temperature = 33.5°C.

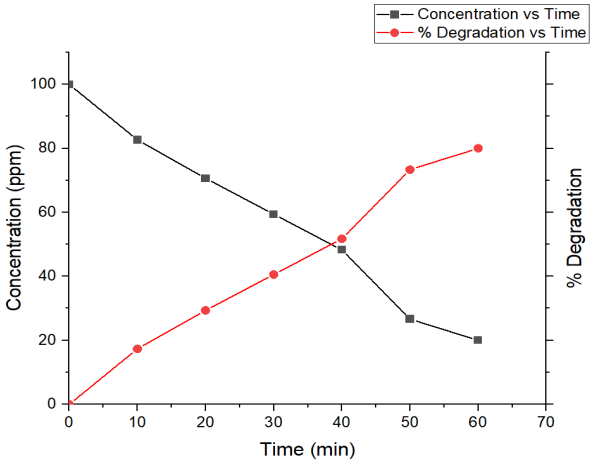

Figure 3. Concentration (ppm) and % degradation vs time (min) for run 14.

Table 1. Values obtained from Experiments conducted vs Predicted values given by RSM software.

Run	Sorted pH	Sorted catalyst dosage	Sorted temperature	Experimental [% deg]	Predicted [% deg]
1	5	5.0	33.5	63.43	63.2200
2	9	5.0	33.5	69.30	70.4000
3	5	30.0	33.5	69.10	69.3100
4	9	30.0	33.5	70.98	72.8700
5	5	17.5	27.0	78.00	78.7900
6	9	17.5	27.0	63.65	63.1000
7	5	17.5	40.0	63.98	64.3000
8	9	17.5	40.0	76.10	75.9367
9	7	5.0	27.0	66.20	67.2000
10	7	30.0	27.0	75.62	75.9367
11	7	5.0	40.0	71.20	72.0900
12	7	30.0	40.0	75.70	75.9367
13	7	17.5	33.5	75.04	75.3400
14	7	17.5	33.5	80.01	79.9200
15	7	17.5	33.5	78.02	76.9800

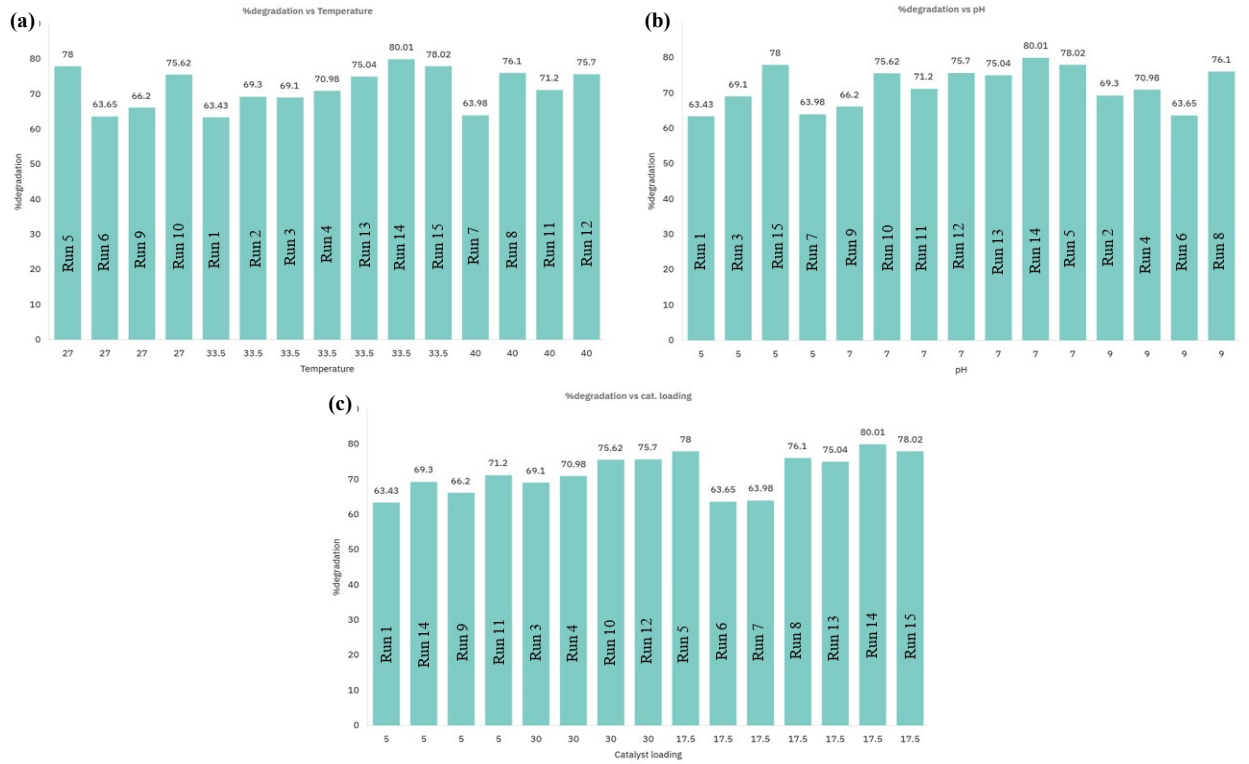

Figure 4. (a) Effect of temperature on degradation efficiency, (b) Effect of pH on degradation efficiency, and (c) Effect of catalyst dosage on degradation efficiency

3.5.1 Effect of temperature on degradation efficiency

It was noted that raising the reaction temperature enhanced the Brown G dye degradation efficiency to a certain optimum level. Based on experimental data and depicted in the response surface plots (Figure 5), the highest performance degradation was attained at a temperature of about 33.5°C, giving a maximum degradation efficiency of 80.01% [20]. Increased temperatures tend to raise the energy of the molecules in the reaction system, leading to a greater frequency and intensity of collisions among dye molecules and on the catalyst surface [10]. Higher temperatures enhance the generation as well as mobility of electron-hole pairs formed in the CuO nanoparticles, which are vital to generate ROS such as hydroxyl radicals (•OH) and superoxide anions ($•O_2^-$) responsible for the degradation of the dye. Temperatures too high will likely result in reduced efficiency as active catalytic sites can become deactivated or there can be greater charge carrier recombination. Hence, keeping the temperature moderately high but within the optimum is important for achieving maximum photocatalytic efficiency without jeopardising catalyst stability and performance. [14].

3.5.2 Effect of pH on degradation efficiency

The pH of the reaction medium is an important factor that affects the surface charge of the CuO nanoparticles, the ionisation state of the dye molecules, and the net generation of reactive oxygen species throughout the photocatalytic degradation process. It can be seen that

at pH 7 produces maximum degradation efficiency of Brown G dye [13]. Additionally, reactive oxygen species formation, like hydroxyl radicals, is most favourable at this pH, thus causing better breakdown of the complicated molecular structure of the dye. Highly alkaline or acidic conditions were linked with lower efficiency in degradation [21]. Under acidic conditions, the charge on the catalyst surface can repel cationic dye species, and under alkaline conditions, charge carrier recombination under photogenerated conditions or the presence of less reactive oxygen species may slow down the degradation process. It is therefore important to keep the solution at or close to neutral pH, not only to maximise the reaction kinetics but also to conserve the structural integrity of the catalyst.

3.5.3 Effect of catalyst dosage on degradation efficiency

From the experimental observations (Table 1) and captured in the contour and surface plots (Figure 5), the degradation efficiency improved with a rise in catalyst loading to an optimal amount of 17.5 mg. At this dosage, the system had the highest degradation efficiency of 80.01%, which is due to the higher number of active sites in the photo-catalytic reaction [13,22]. With a higher concentration of catalyst particles, there will be better absorption of UV light and the creation of more electron-hole pairs, which results in a higher production of reactive oxygen species that degrade the dye. However, beyond the optimal dose (e.g., 30 mg), the efficiency of degradation improved little or was even decreased. This decrease can be due to light scattering and screening effects due to an excess amount of catalyst particles [10]. If the concentration of the nanoparticles is too high, the nanoparticles can agglomerate or prevent the UV light from penetrating the reaction mixture, which in turn limits the activation of further catalyst surfaces [23]. In addition, excessive catalyst loading can cause increased recombination of charge carriers, lowering ROS formation efficiency. Hence, although it is important to ensure there is enough catalyst for effective degradation, too much can be unfavourable [24,25].

3.5.4 Analysis of variance

Table 2 shows the Analysis of Variance data for the experiments carried out from RSM [17,19]. The variables such as Degrees of Freedom (DF), Adjusted Sum of Squares (Adj SS) (higher values indicate greater influence on the response), and Adjusted Mean Square value (Adj MS) are given in a table. The ratio of Adj MS of the data to the Adj MS of the error was given as the F-Value, and the Probability of the F-Value occurring is given as the P-Value.

It can be observed from the table that the P-values of all the data (except Lack of Fit) are < 0.001. For a model to be stable, the P-values of all variables must be ≈ 0, and the value of Lack-of-Fit must be > 0.1. Hence, it can be observed that from the results, the given model is stable [26].

The regression equation for the model can be given by the Equation (2):

$$\%\ \text{Degradation} = 53.27 + 12.524\,x - 3.0508\,y + 0.2618\,z - 1.4235\,x^{*}x - 0.005499\,y^{*}y - 0.04300\,z^{*}z + 0.14920\,x^{*}y + 0.16865\,x^{*}z + 0.070923\,y^{*}z$$

Where x is pH, y is Catalyst dosage, and z is Temperature.

3.6 Contour plots

It can be observed from Figure 9 that the degradation efficiency increases with an increase in catalyst dosage and with the pH being more neutral. From the results, the highest efficiency was achieved at a pH of 7 and a catalyst amount of 17.5 mg. It can also be observed that we obtain very close values in the runs where a similar or larger amount (30 mg) of catalyst is used at a similar pH of 7. The dark green zones denote the conditions where maximum degradation efficiency is expected, and blue zones denote the conditions where the least efficiency is expected [26].

Table 2. Analysis of variance.

Source	DF	Adj SS	Adj MS	F-Value	P-Value
Model	9	410.663	45.629	3576.42	<0.001
Linear	3	75.791	25.264	1980.17	<0.001
pH	1	23.427	23.427	1836.21	<0.001
Catalyst dosage	1	39.206	39.206	3072.93	<0.001
Temperature	1	13.158	13.158	1031.36	<0.001
Square	3	127.166	42.389	3322.43	<0.001
pH*pH	1	119.718	119.718	9383.49	<0.001
Catalyst dosage*Catalyt	1	2.726	2.726	213.63	<0.001
Dosage					
Temperature	1	12.186	12.186	955.11	<0.001
2-Way Interaction					
Temperature*Temperature	3	207.705	69.235	5426.66	<0.001
pH*Catalyst dosage	1	55.652	55.652	4361.98	<0.001
pH*Temperature	1	19.228	19.228	1507.11	<0.001
Catalyst dosage*Temperature	1	132.826	132.826	10410.89	<0.001
Error	5	0.064	0.013		
Lack-of-Fit	3	0.057	0.019	5.53	0.157
Pure Error	2	0.007	0.003		
Total	14	410.726			

(a) Contour plot of % degradation vs catalyst dosage, pH

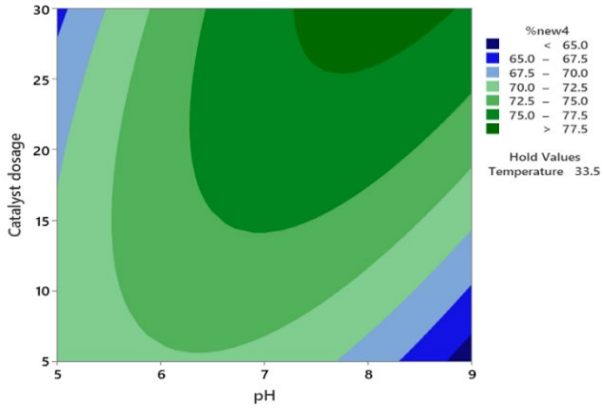

(b) Contour plot of % degradation vs temperature, catalyst dosage

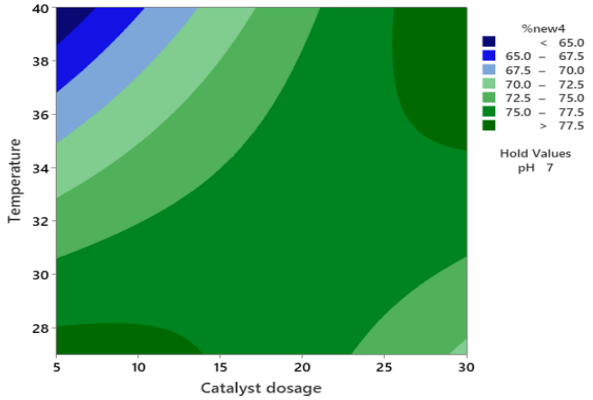

(c) Contour plot of % degradation vs temperature, pH

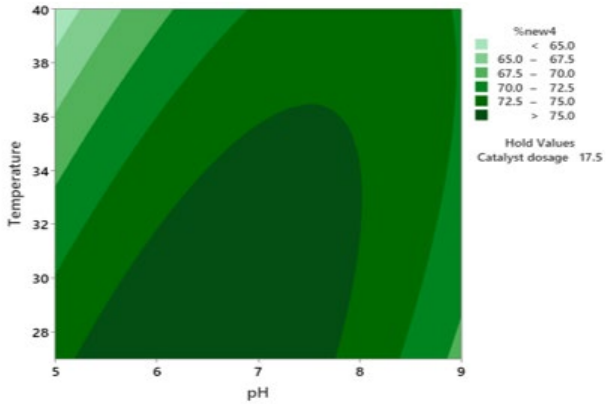

(d) Surface plot of % degradation vs temperature, catalyst dosage

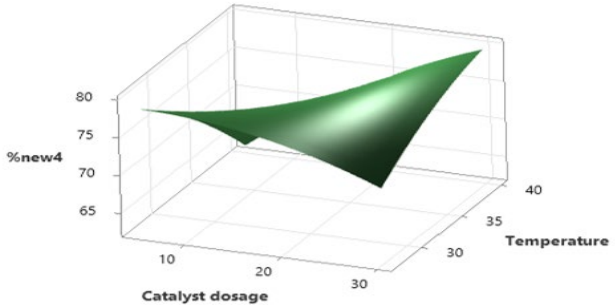

(e) Surface plot of % degradation vs temperature, pH

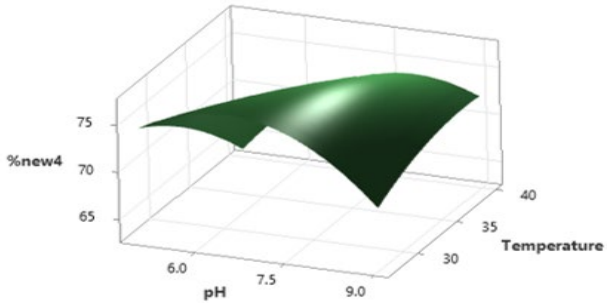

Figure 5. (a) Contour plot of % degradation vs catalyst dosage and pH, (b) Contour plot of % degradation vs temperature and catalyst dosage, (c) Contour plot of % degradation vs temperature and pH, (d) Surface plot of % degradation vs temperature and catalyst dosage, and (e) Surface plot of % degradation vs temperature and pH.

Figure 5(b) shows the interaction between temperature and catalyst dosage on degradation efficiency. As the temperature increases gradually, an increase in catalyst loading is needed for the degradation efficiency to be optimum. The dark green regions denote maximum degradation efficiency, and the blue regions denote lesser degradation efficiency. From our experiments, the maximum efficiency of 80.01% was obtained at a Temperature of 33.5°C and a Catalyst Loading of 17.5 mg. Similar values were obtained at 30 mg loading as well [26,27].

Figure 5(c) shows the contour plot of the effect of temperature and pH on degradation efficiency. We can observe that as the temperature reaches a moderate value, the change in pH towards a more neutral value causes the degradation efficiency to significantly increase. The dark green zones represent the conditions where the degradation efficiency is expected to be maximum. The light green zones denote lesser degradation efficiency [26].

3.7 Surface plots

Figure5(d) shows the surface plot of the effect of temperature and catalyst dosage on degradation efficiency. The highest points in the 3D curve represent the conditions where the efficiency is maximum. The lower points on the 3D curve depict the lower efficiencies [26]. Figure 5(e) shows the effect of Temperature and pH on percentage degradation. From the figure, it can be observed that the higher regions show the areas of maximum efficiency on simulation, and the lower points in the plot show areas of lesser efficiency [19,26].

Table 3. Regression calculations.

S	R-sq	R-sq(adj)	R-sq(pred)
0.112953	99.77%	99.96%	99.98%

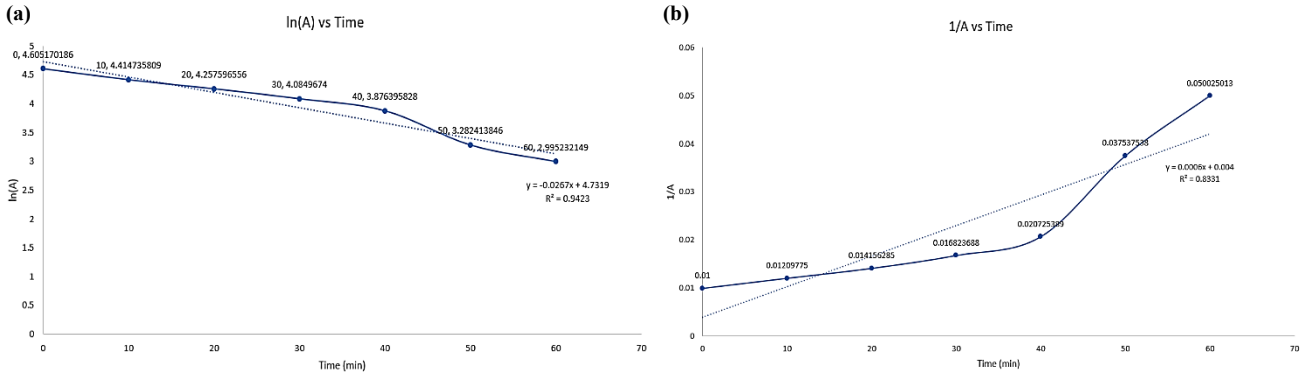

Figure 6. (a) First-order kinetics for Run 14, (b) Second-order kinetics for Run 14 (Initial Concentration: 100 ppm, Temperature = 33.5°C, pH = 7, Catalyst Dosage = 17.5mg)

3.8 Regression analysis

From the simulation model, we can analyse the results given by the software and the results are shown in Table 3. It shows the values of standard deviation (S), actual regression value (R^2), and regression value predicted by the software (R^2 (pred)).

The standard deviation value has to be as low as possible, and the calculated regression values should be more than 99 % to prove the simulation is a stable model. We can confirm that the model is stable from the obtained values [23].

3.9 Kinetic studies

We could observe from the results given by RSM that the R^2 value for the given degradation model is very high. First-order and second-order kinetics studies were carried out for the degradation process, and Run 14 data were used to calculate the kinetics of the reaction, as shown in Figure 6(a-b).

From the figure, the first-order and second-order rate constant (k) values of 0.0267 s^{-1} and 0.0006 $L \cdot mol^{-1} \cdot s^{-1}$ were obtained with the R^2 values of 0.942 and 0.8335, respectively. From the results, it was concluded that degradation of Brown G follows first-order kinetics

4. Conclusion

This study focuses on the successful green synthesis of copper oxide (CuO) nanoparticles using coconut coir extract as a natural reducing and stabilising agent. This eco-friendly method aligns with green chemistry principles and promotes agricultural waste reuse, supporting a circular economy. The CuO nanoparticles synthesised in this study are distinct due to the use of coconut coir extract - an underutilised, low-cost biowaste rich in natural reducing and stabilising agents. This results in stable nanoparticles with effective photocatalytic performance. The green sol–gel route adopted here is easily scalable under mild conditions, making it economically and environmentally viable for industrial wastewater treatment applications. Characterisation through XRD and FTIR confirmed the crystalline structure and presence of Cu–O bonds. The CuO nanoparticles showed strong photocatalytic activity under UV light, effectively degrading the persistent azo dye Brown G through the generation of reactive oxygen species (ROS), such as hydroxyl and superoxide radicals. To optimise the process, Response Surface Methodology (RSM) was used to determine ideal conditions including catalyst dosage, pH, dye concentration, and UV exposure time to maximize efficiency while reducing experimental trials. The maximum degradation efficiency of 80.01% was obtained at a temperature of 33.5°C and a catalyst loading of 17.5 mg, and at a pH of 7. Also, kinetics studies show that the degradation follows first-order kinetics. In conclusion, this study presents a sustainable and efficient approach to wastewater treatment by combining green nanotechnology, photocatalysis, and statistical optimisation. Future research should focus on the reusability of CuO NPs, their performance under visible or natural light, and integration into large-scale treatment systems.

Acknowledgements

We express our appreciation to VIT University for offering a stimulating academic environment and access to resources that greatly supported our learning and project work. We are also thankful to the faculty and staff of the Chemical Engineering Department, SCHEME, for providing us with the necessary resources and laboratory facilities to carry out our research effectively. Their assistance has been essential in overcoming challenges and achieving our project objectives.

References

[1] M. P. Niharika, R. Garlapallya, K. Ruthvik, M. Velaga, and B. Manmadha Rao, "Hydrogen production on g-C_3N_4 nanoflakes via photoelectrochemical water splitting," *Materials Today: Proceedings*, 2023

[2] M. Mathanmohun, S. Sagadevan, Md Z. Rahman, J. A. Lett, I. Fatimah, S. Moharana, S. Garg, and M. A. Al-Anber, "Unveiling

sustainable, greener synthesis strategies and multifaceted applications of copper oxide nanoparticles," *Journal of Molecular Structure*, vol. 1305, p. 137788, 2024.

[3] K. R. Kaja, S. A. Behera, B. Das, S. Hajra, S. Panda, M. A. Belal, N. Vittayakorn, B. Nanda, P. G. R. Achary, and H. J. Kim, "Calcium copper titanate particles based energy harvesting and removal of pharmaceutical pollutants," *ACS Applied Electronic Materials*, vol. 7, no. 9, pp. 4327–4338, 2025.

[4] A. Panda, K. K. Das, K. R. Kaja, V. Gandi, S. G. Mohanty, and B. K. Panigrahi, "Low-cost high performance sustainable triboelectric nanogenerator based on laboratory waste," *Journal of Metals, Materials and Minerals*, vol. 35, no. 1, p. e2226, 2025.

[5] C. Madhusha, T. Jauasundara, I. Munaweera, C. Perera, G. Wijesinghe, M. Weerasekera, C. Sandaruwan, A. Meiyazhagan, F. C. R. Hernandez, P. M. Ajayan, and N. Kottegoda, "Synthesis and structural characterization of copper nanoparticles doped activated carbon derived from coconut coir for drinking water purification," *Materials Today Chemistry*, vol. 27, p. 101312, 2023.

[6] A. Panda, K. K. Das, K. R. Kaja, M. Belal, and B. K. Panigrahi, "Single electrode mode triboelectric nanogenerator for recognition of animal sounds," *Journal of Metals, Materials and Minerals*, vol. 34, no. 4, p. 2170, 2024.

[7] M. D. Moroda, T. Leta Deressa, A. H. Tiwikrama, and T. F. Chala, "Green synthesis of copper oxide nanoparticles using Rosmarinus officinalis leaf extract and evaluation of its anti-microbial activity," *Next Materials*, vol. 7, p. 100337, 2025.

[8] N. Chakraborty, J. Banerjee, P. Chakraborty, A. Banerjee, S. Chanda, K. Ray, K. Acharya, and J. Sarkar, "Green synthesis of copper/copper oxide nanoparticles and their applications: A review," *Green Chemistry Letters and Reviews*, vol. 15, no. 1, pp. 187–215, 2022.

[9] H. N. Jayasimha, K. G. Chandrappa, P. F. Sanaulla, and V. G. Dileepkumar, "Green synthesis of CuO nanoparticles: A promising material for photocatalysis and electrochemical sensor," *Sensors International*, vol. 5, p. 100254, 2024.

[10] H. Ahsan, M. Shahid, M. Imran, F. Mahmood, M. H. Siddique, H. M. Ali, M. B. K. Niazi, S. Hussain, M. Shahbaz, M. Ayyub, and T. Shahzad, "Photocatalysis and adsorption kinetics of azo dyes by nanoparticles of nickel oxide and copper oxide and their nanocomposite in an aqueous medium," *Biochemistry, Biophysics and Molecular Biology*, vol. 10, e14358, 2022.

[11] N. M. Mahmoodi, M. Arami, N. Y. Limaee, and N. S. Tabrizi, "Kinetics of heterogeneous photocatalytic degradation of reactive dyes in an immobilized TiO_2 photocatalytic reactor," *Journal of colloid and interface Science*, vol. 295, no. 1, pp. 159-164, 2006.

[12] A. Fujishima and K. Honda, "Electrochemical photolysis of water at a semiconductor electrode," *Nature*, vol. 238, no. 5358, pp. 37–38, 1972.

[13] M. A. Rauf, and S. S. Ashraf, "Fundamental principles and application of heterogeneous photocatalytic degradation of dyes in solution," *Chemical engineering journal*, vol. 151, no. 1-3, pp. 10-18, 2009.

[14] J. Komara, J. P. Karumuri, and B. S. S. Naik, "Green synthesis of copper oxide nanoparticles using solanum melongena seeds extract and its applications in degradation of Rose Bengal dye, antibacterial, catalytic reduction and antioxidant activity," *Hybrid Advances*, vol. 7, p. 100304, 2024.

[15] T. Gayathri, S. L. Kumar, S. Sangavi, M. Yudhika, &and M. Swathy, "Green synthesis of copper oxide nanoparticles using Carica papaya and their antimicrobial activity," *Materials Today: Proceedings,* 2023.

[16] F. H. Hussein, A. F. Halbus, H. A. K. Hassan, and W. A. K. Hussein, "Photocatalytic degradation of bismarck Brown G using irradiated ZnO in aqueous solutions," *Journal of Chemistry*, vol. 7, no. 2, pp. 540–544, 2010.

[17] A. I. Khuri, and S. Mukhopadhyay, "Response surface methodology, Wiley interdisciplinary reviews," *Computational statistics*, vol. 2, no. 2, pp. 128-149, 2010.

[18] R. H. Myers, "Response surface methodology—current status and future directions," *Journal of quality technology*, vol. 31, no. 1, pp. 30-44, 1999.

[19] J. P. Kleijnen, "Response surface methodology for constrained simulation optimization" An overview," *Simulation Modelling Practice and Theory*, vol. 16, no. 1, pp. 50-64, 2008.

[20] A. Houas, H. Lachheb, M. Ksibi, E. Elaloui, C. Guillard, and J-M. Herrmann, "Photocatalytic degradation pathway of methylene blue in water," *Applied Catalysis B: Environmental*, vol. 31, no. 2, pp. 145-157, 2001.

[21] M. Jeevarathinam, and I. V. Asharani, "Synthesis of CuO, ZnO nanoparticles, and CuO-ZnO nanocomposite for enhanced photo-catalytic degradation of Rhodamine B: A comparative study," *Scientific Reports*, vol. 14, no. 1, p. 9718, 2024.

[22] K. Dulta, G. K. Agceli, P. Chauhan, R. Jasrotia, P. K. Chauhan, and J. O. Ighalo, "Multifunctional CuO nanoparticles with enhanced photocatalytic dye degradation and antibacterial activity," *Sustainable Environment Research*, vol. 32, pp. 1-15, 2022.

[23] S. Korpe, B. Bethi, S. H. Sonawane, and K. V. Jayakumar, "Tannery wastewater treatment by cavitation combined with advanced oxidation process (AOP)," *Ultrasonics Sonochemistry*, vol. 59, p. 104723, 2019.

[24] S. Jiménez, M. Andreozzi, M. M. Micó, M. G. Álvarez, and S. Contreras, "Produced water treatment by advanced oxidation processes," *Science of The Total Environment*, vol. 666, pp. 12–21, 2019.

[25] I. M. F. Cardoso, R. M. F. Cardoso, and J. C. G. E. da Silva, "Advanced oxidation processes coupled with nanomaterials for water treatment," *Nanomaterials*, vol. 11, no. 8, p. 2045, 2021.

[26] A. T. Nair, A. Makwana, and M. M. Ahammed, "The use of response surface methodology for modelling and analysis of water and wastewater treatment processes: A review," *Water science and technology*, vol. 69, no. 3, pp. 464-478, 2014.

[27] S. J. M. Breig, and K. J. K. Luti, "Response surface methodology: A review on its applications and challenges in microbial cultures," *Materials Today: Proceedings*, vol. 42, pp. 2277-2284, 2021